

Simultaneous optimization and simulation of multi-purpose reservoir operation rule curves under extreme hydrological conditions and complex cultivation patterns using evolutionary algorithms

Farzane Karami 

Ghods Niroo Consulting Engineering Company, Tehran, Iran.
Email: farzane_krm@yahoo.com




Abstract

Implementing appropriate operating rule curves for water resources systems and hydroclimatic conditions significantly reduce damages floods and droughts damages in the downstream area. This paper uses simulation-optimization approach to establish a multi-purpose reservoir's rule curve. The hedging method is utilized for drought, and the multi-stage flood routing method is used for floods. The melody search algorithm is employed as the optimization algorithm. The Karkhe Reservoir is a case study, facing irregular water distribution and hydrological challenges from extensive domestic and agricultural water usage, varying cultivation patterns, and flood susceptibility. The region grows two types of crops - autumn and summer crops. Autumn cultivation is fundamental and strategic, but water use for summer or water-based crops reduces water resources for it. Meeting water demands from September to November is another challenge due to the overlapping water needs of summer and autumn crops. Significant changes in the upstream and downstream areas, including alterations in the shape and water resource utilization of the catchment area, as well as changes in the rivers' morphological condition and water carrying capacity, make it a constant challenge to determine the optimal water level for the reservoir. The results demonstrate the satisfactory performance of the optimized rule curve.

Keywords: Cultivation pattern, Hedging, Heuristic algorithms, Multi-stage flood routing method, Reservoir's rule curve, Simultaneous simulation-optimization approach.

Citation | Karami, F. (2025). Simultaneous optimization and simulation of multi-purpose reservoir operation rule curves under extreme hydrological conditions and complex cultivation patterns using evolutionary algorithms. *World Scientific Research*, 12(1), 32-45, 10.20448/wsr.v12i1.6791

History:
Received: 26 March 2025
Revised: 6 May 2025
Accepted: 10 June 2025
Published: 16 June 2025

Licensed: This work is licensed under a [Creative Commons Attribution 4.0 License](#) 

Publisher: Asian Online Journal Publishing Group

Funding: This study received no specific financial support.

Institutional Review Board Statement: Not Applicable

Transparency: The author confirms that the manuscript is an honest, accurate, and transparent account of the study; that no vital features of the study have been omitted; and that any discrepancies from the study as planned have been explained. This study followed all ethical practices during writing.

Data Availability Statement: Farzane Karami may provide study data upon reasonable request.

Competing Interests: The author declares that there are no conflicts of interests regarding the publication of this paper.

Contents

1. Introduction	33
2. Methodology	33
3. Case Study	36
4. Results	39
5. Conclusion	44
References	44

Contribution of this paper to the literature: This study uniquely combines hedging for drought and multi-stage flood routing within a simulation-optimization framework using the melody search algorithm to establish an effective rule curve for the complex Karkhe Reservoir system facing diverse challenges, effectively addressing water allocation across normal, drought, and flood conditions within its complex agricultural-hydrological context.

1. Introduction

The rule curve is a tool for reservoir operation, dividing the storage volume into zones where different strategies for demand-supply are applied. The difference lies in their politics. Some, like the yield model's rule curves, prioritize demands and supply risk percentage. Some are used in times of crisis, such as drought and severe water shortages [1].

The simplest operating rule curve is the standard operating policy (SOP). In this policy, release from the reservoir is determined based on the demands of each period. If there is not enough water to meet the demands, the reservoir will be empty, and if there is more water available, it will be filled and then spilled. However, this model lacks the necessary foresight for efficient reservoir management.

Another common method in water resources management is the use of hedging laws during a drought period or approaching a drought. In this method, even though it is possible to provide the entire demand, sometimes only a part of it is provided Bayesteh and Azari [2]. Hashimoto, et al. [3] presented the first hedging method. Bayazit and Ünal [4] explored the determination of hedging parameters in reservoir exploitation. Shih and ReVelle [5] subsequently proposed the single-point hedging method, where the reservoir output gradually increases from the origin with a slope less than one until meeting the demand line. Shih and ReVelle [6] also introduced the discrete hedging method.

On the other hand, reservoir management faces a major challenge in operating spillway gates during a flood. If a spillway gate is opened too much, it releases a large flow that can cause downstream damages. Conversely, if the gates are not opened enough, it can seriously threaten the dam's safety Zargar, et al. [7]. Acanal and Haktanir [8]; Acanal, et al. [9] and Haktanir and Kisi [10] devised a flood control operation policy suitable for all flood hydrographs, regardless of magnitude (from Small to the PMF), in the absence of flood forecasts. In their studies, the flood retention storage of the reservoir was divided into multiple levels (five, six and ten stages), and the gate openings at these levels were determined through trial and error. This method leads to a high number of potential operation alternatives, which may not include the global optimum. Salehi, et al. [11] developed spillway operation rules to safely and efficiently manage floods of all sizes through the reservoir, while reducing human errors caused by stress during flood operations. The proposed approach enhances the ten-stage strategy put forward and tested by Haktanir and Kisi [10] within a simulation-optimization framework. Su, et al. [12] examined the optimal flood control operation for reservoirs, taking into account spillway gate scheduling.

It is inevitable to use new tools and methods to solve the problems of optimizing water resources systems. Over the past four decades, numerous algorithms have been created to address different engineering optimization issues include ant colony, genetic, annealing simulation and harmony and melody search algorithms. Geem, et al. [13] developed a harmony search (HS) algorithm based on the phenomenon of "musical harmony". This algorithm was later improved by various researchers [14-18]. Finally, Ashrafi and Dariane [19] introduced the melody search algorithm, inspired by the harmony search algorithm.

In this article, a simulation-optimization approach is developed to establish the reservoir's rule curve during drought and flood situations. The hedging method was modified for drought considering the irregularity in the water distribution entering, cultivation pattern and several hydrological issues. On the other hand, the multi-stage flood routing method was modified for flood considering not only the typical reservoir constraints but also the operation constraints of each spillway gate, as well as the impact of the reservoir water level and gate opening degree on discharge capacity.

2. Methodology

2.1. Discrete Hedging Method

The hedging method causes water storage and acceptance of a small shortage in the current period to reduce severe shortages in the future, which is important from economic and social perspectives. During droughts, farmers are more likely to experience a series of smaller shortages rather than one severe, catastrophic period. By applying the hedging rule, water shortage is spread out over a longer period, improving the efficiency of reservoir usage.

In the discrete hedging method (Figure 1), V_1 , V_2 , and V_3 for each month (p) specify the hedging phases [6]. As can be seen in this figure, whenever the sum of storage and delivery water for each specific month p is greater than V_{1P} , all the demands are met. However, if the total storage and delivery water is less than V_{1P} and more than V_{2P} , only α_1 percent of the requirement is provided and it is called the first phase of hedging, and in the same way, if the total storage and delivery water is less than V_{2P} and more From V_{3P} , α_2 percent of the requirement is provided and it is called the second phase of hedging [20].

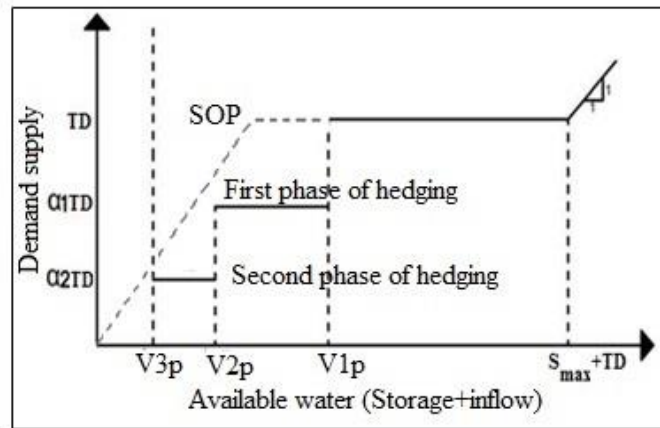


Figure 1. Discrete hedging rule.

2.2. Multi-Stage Flood Routing

Reservoir management faces a significant challenge with operating spillway gates during floods. Opening a gate too wide can release a dangerous amount of water, bypassing the reservoir's flood control capacity and causing downstream damage. Conversely, inadequate gate opening can compromise the dam's safety. This paper uses the multi-stage flood routing method for gated reservoirs to determine flood management. The main idea of this method is that the anticipated future flood, in terms of volume and peak, falls within the range of the `.

To achieve this goal, flood routing in the reservoir begins with 2-year return period flood and then follows the single exploitation policy until the dam design flood is reached. The routing results from the previous period are used to determine the routing for the next period. Prior to commencing the simulation, the critical levels' locations must be inputted into the model. These levels are denoted by H in the following. Figure 2 provides a schematic representation of the critical levels' positions and the discharge for each step.

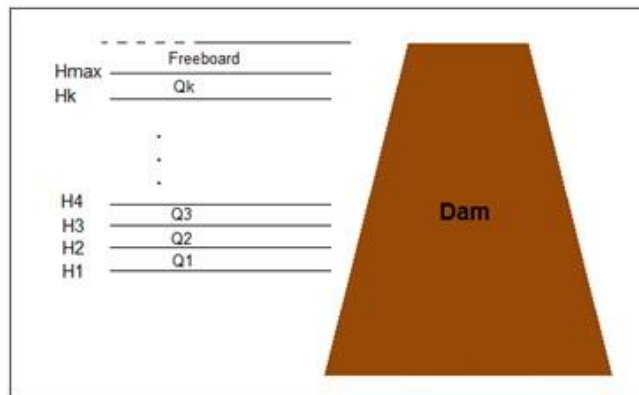


Figure 2. schematic representation of the critical levels' positions.

After identifying the critical levels, it is important to establish a consistent flow through various stages. This consistent flow at each stage is referred to as the critical flow. The primary consideration in determining critical discharges is to utilize the reservoir's maximum capacity for flood control. This means ensuring that the valve opening is not so low that the dam would be bypassed by floods, particularly the design flood, and not so high that it would cause downstream damage without utilizing the reservoir's flood storage capacity. The output flow at each stage is chosen to ensure that the dam's spillway has the capacity to handle it.

After determining the output discharge, it is important to ensure that the discharge of each step does not exceed the flow rate obtained from the stage-discharge relation. Additionally, the output flow from each step in the ascending branch of the hydrograph should be greater than or equal to the flow of the previous step. The primary objective is to identify the critical discharges. To accomplish these goals and establish the decision-making variables, the following equations are utilized.

$$Q_1 = \alpha_1 Q_{max_1} \quad (1)$$

$$Q_2 = Q_1 + \alpha_2 (Q_{max_2} - Q_1). \quad (2)$$

$$Q_k = Q_{k-1} + \alpha_k (Qmax_k - Q_{k-1}) \quad (3)$$

In these equations, k is the index of the critical level number, Q_k is the critical output flow in the K th step and Q_{max_k} is the maximum flow passing through the spillway with fully open valves in the K th step. α_k is a coefficient between zero and one, which is determined through optimization modeling. The equations present the method for calculating the critical flow in the first, second, and k th steps, respectively, using the flow relation of the dam.

Given the known values of Q_{max_k} and Q_{k-1} the only coefficient α_k remains unknown for determining the flow rate of each step. These coefficients are obtained through the optimization process. Hence, the number of decision variables depends on the number of steps. To constrain the decision-making space of the optimization problem, the coefficient α_k is limited to a range between zero and one. In the aforementioned relationships, selecting α_k as zero equates the discharge of the new step to that of the previous step. When α_k zero in the first step, the outflow is zero, indicating the maintenance of closed spillway valves. Conversely, choosing α_k as one results in the outflow of the new step matching the maximum spillway capacity, assuming fully open valves in that step.

To calculate the flood routing in the reservoir, the following continuity relationship is employed, where $I(t)$ and $O(t)$ denote the inflow and outflow rates, $S(t)$ signifies the reservoir volume, and $dS(t)/d(t)$ is the rate of reservoir volume change at time t .

$$I(t) - O(t) = dS(t) / d(t) \quad (4)$$

Using the finite difference method, equation 9 can be broken down as follows.

$$S_t = S_{t-1} + \frac{I_{t-1} + I_t}{2} \Delta t - \frac{O_{t-1} + O_t}{3} \Delta t \quad (5)$$

In this equation, Δt signifies the time step, and t and $t-1$ represent the present and past time. The equation above contains two unknowns O_t and S_t . Initially, the reservoir's water level equals the normal level during flood seasons, and the discharge from the reservoir in the first simulation step equals the discharge of the initial step. Once the storage of the reservoir is calculated, the corresponding water level is determined as well.

After calculating the level of h_t , a decision is made by comparing it with critical levels and determining the output flow rate from the reservoir based on the following equations.

At the beginning.

$$\begin{cases} \text{if: } h_t = Hcr_1 \text{ and } I_t < Qcr_1 & \Rightarrow O_t = I_t \\ \text{if: } h_t = Hcr_1 \text{ and } I_t \geq Qcr_1 & \Rightarrow O_t = Qcr_1 \end{cases} \quad (6)$$

In the rising limb.

$$\begin{cases} \text{if: } h_t < Hcr_{(k+1)} & \Rightarrow O_t = Qcr_k \\ \text{if: } h_t \geq Hcr_{(k+1)} \text{ and } h_t < H \max & \Rightarrow O_t = Qcr_{k+1} = Qcr_k + \alpha_{k+1} (Q \max_{k+1} - Qcr_k) \\ \text{if: } h_t \geq Hcr_{(k+1)} \text{ and } h_t < H \max \text{ and } Qcr_{k+1} > I_t & \Rightarrow O_t = Qcr_{k+1} = I_t \end{cases} \quad (7)$$

In the recession limb.

$$\begin{cases} \text{if: } h_t < Hcr_k & \Rightarrow O_t = Qcr_{k-1} \\ \text{if: } h_t \leq Hcr_k \text{ and } I_t > Qcr_{k-1} & \Rightarrow O_t = I_t \end{cases} \quad (8)$$

Based on the equations above, if the reservoir water level remains below the critical level of the next step ($Hcr_{(k+1)}$), the output flow rate from the reservoir remains unchanged and equals the flow rate of the k th step (Qcr_k). The calculations continue in this manner until the reservoir water level reaches or exceeds the critical level of the next step ($Hcr_{(k+1)}$).

If the reservoir water level is greater than or equal to the critical level of the next step ($Hcr_{(k+1)}$) the reservoir has reached the next critical level in a time less than Δt . Consequently, the precise time of transition to the next level is calculated, and the outflow from the reservoir equals the critical flow of the next step. Furthermore, in the ascending branch of the hydrograph, the flow rate calculated for each step must be less than or equal to the flow rate entering the reservoir when the water level of the reservoir reaches that step. These calculations continue until the completion of the ascending branch of the output hydrograph. Following this phase, the descending branch of the output hydrograph commences, and the reservoir level gradually decreases.

Flood routing in the descending branch follows the same principles as in the ascending branch, with the distinction that in the descending branch, when the water level of the reservoir is less than or equal to the critical level of the k th step (Hcr_k) the flow through the spillway will be equal to the critical flow of the lower step. It should be noted that in the descending branch of the hydrograph, to prevent fluctuation in the reservoir water level when the water level reaches a lower step with a critical flow rate less than the inflow, the outflow should be equal the inflow.

Finally, the Karkhe reservoir was divided into one-meter increments from the normal level, i.e. 220 to 229. It should be noted that the upper level of the valves in the fully closed state is 226.25 meters above sea level. If the water level of the reservoir exceeds 226, the spillway valves should be opened to prevent bypassing the valve. Therefore, up to level 226, the output flow from the spillway of the Karkhe can be controlled by opening the overflow valves. Beyond this level, the water level of the reservoir determines the amount of opening, and after the level of 226, the outflow from the spillway will increase significantly.

2.3. Simulation-Optimization Approach

In this study, the optimal rule curve or operation policy has been prepared by combining optimization and simulation algorithms. In this approach, after the decision variables are determined by the optimizer algorithm, the system is simulated with the determined decision variables. After the simulation, the performance of the system is evaluated and the results are returned to the optimizer algorithm [21]. In the optimizer algorithm, the decision variables are updated again according to the values of the evaluation criteria. These updated decision variables are again sent to the simulation algorithm and the same process is repeated until the end of the program. Therefore, in each step, the feedback of the previous step is used to improve the solution and the model is tried to be guided towards the optimal solution. The results are applied again in the simulation model and this process is repeated until reaching a suitable solution (Figure 3).

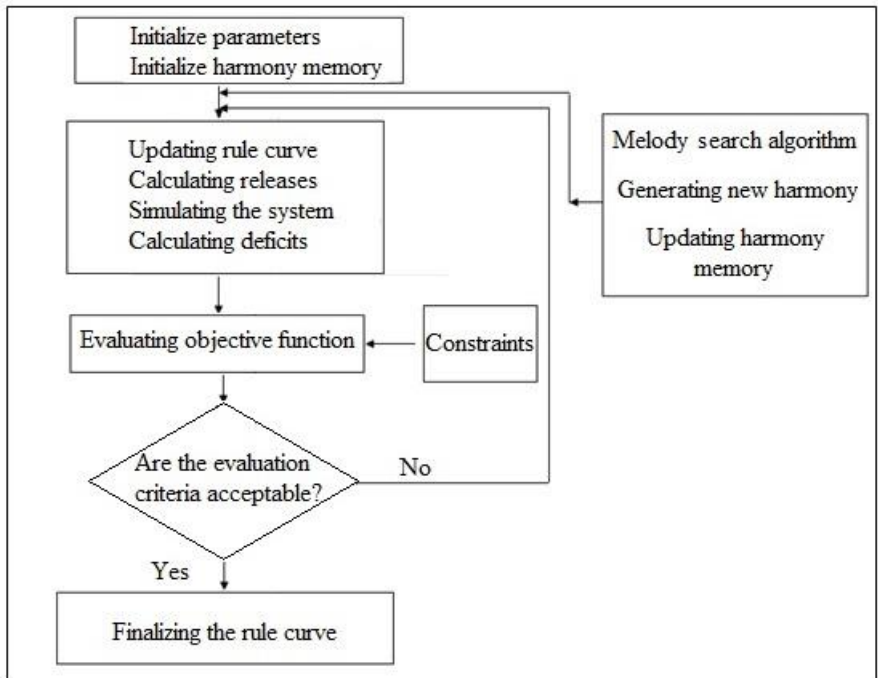


Figure 3. Simulation-optimization approach.

In this study, melody search algorithm is used for optimization. The parameters of the algorithm are the harmony memory size (HMS which indicates the number of solution in the harmony memory, harmony memory considering rate (HMCR), pitch adjusting rate (PAR), and the number of improvisations (NI). Melody search algorithm consists of two phases. In the initial phase of the calculations, the musicians independently reach an acceptable melody and memories are optimized individually. They are then sorted based on objective function values. The new harmony is generated based on memory consideration, pitch adjustment and random selection rules. The new answer is selected by the probability of the Harmony Memory consideration Rate (HMCR) from within the Harmony Memory (Equation 1) and with the probability (1-HMCR) of all allowed values between lower (LB) and upper (UP) bounds for each decision variable which is indicated by the index i (Equation 9). If the new answer is selected from within the Harmony Memory, it is pitch-adjusted by the probability of the Pitch Adjustment Rate (PAR) (Equation 10). The adjustment is made using the arbitrary distance bandwidth (bw) which is changed dynamically with generation number as shown in (Equation 11). The maximum and minimum of bw are determined by the user for each decision variable through sensitivity analysis. Finally, if the new answer is better than the worst memory, it replaces it. This process continues until the initial phase is finished [19, 22].

$$X_{new}(i) = X_a(i) \quad (9)$$

$$X_{new}(i) = LB_i + r * (UB_i - LB_i) \quad (10)$$

$$X_{new}(i) = X_{new}(i) \pm b_w * Random \quad (11)$$

$$b_w(t) = \begin{cases} b_{w,max} - \frac{b_{w,max}-b_{w,min}}{NI} * 2t & , \text{if } t < NI/2 \\ b_{w,min} & , \text{if } t > NI/2 \end{cases} \quad (12)$$

The second phase involves group calculations. In this stage, the best answers from each memory are compared to determine the minimum and maximum values for the allowed intervals of random production. In each subsequent calculation step, the best solutions from all memories are first identified, and then the lowest and highest values of each decision variable from the best available solutions are chosen as the new limits for the respective variable.

3. Case Study

3.1. Karkhe Watershed

The Karkhe watershed extends from 46° -23' to 49°-12' eastern longitude and 33°-40' to 35°-00' northern latitude. The Karkhe River has a total of 274 main and tributary rivers, with a combined length of 7701 km. Figure 4 depicts the location map of the system under study. As mentioned, the Hoor-ol-Azim Lagoon is located at the end of the basin. The length of the Hoor-ol-Azim wetland is about 100 km and its width is between 15-75 km. It is limited from the west by the Tigris River and from the east by the flat plains of Iran. Throughout, the Hoor is covered by reeds. The depth of the water towards the sides is shallow while in the center it is more than 7 m.

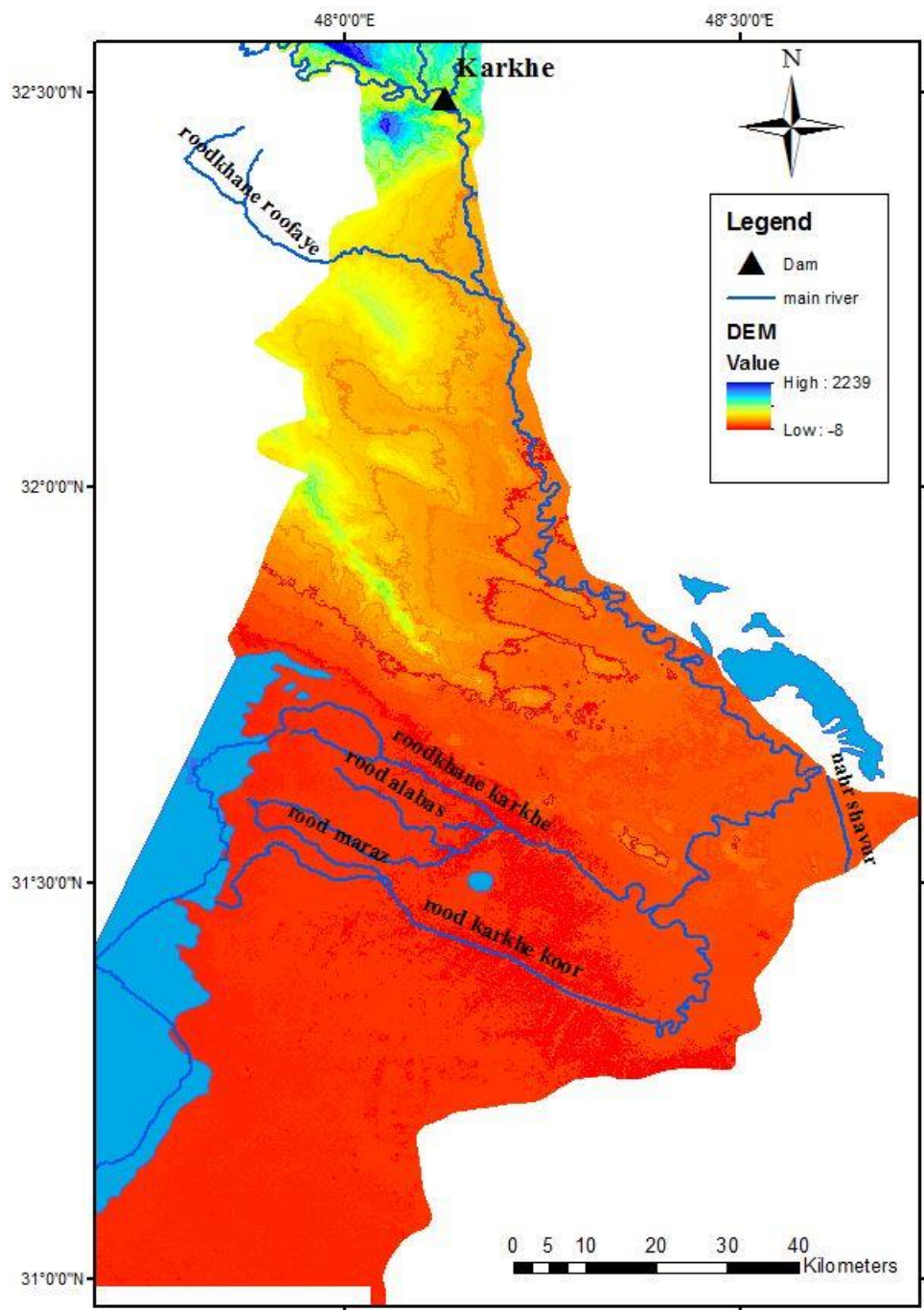


Figure 4. April 2018 flood routing.

Examining the long-term time series of the Karkhe watershed reveals the irregularity in the water distribution entering the Karkhe dam and several hydrological issues throughout the time series. Downstream of the Karkhe Dam, the water resources system of the Karkhe basin exhibits unique characteristics. One of the challenges in the basin is the cultivation pattern. The region grows two types of crops - autumn and summer crops. Autumn cultivation is fundamental and strategic, but at times, using water for summer crops or cultivation of water-based crops such as rice in summer reduces water resources for autumn cultivation. Meeting water demands from September to November is another challenge due to the overlapping water needs of summer and autumn crops, putting pressure on limited water resources. On the other hand, the Karkhe River passes through areas with diverse morphologies, leading to changes in its bed slope. This area is prone to flooding, and in recent years, floods have caused significant damage to the province's infrastructure, highlighting the importance of addressing this issue. Consequently due to the widespread distribution of water resource users, the reliance of a large part of the province on the basin's water resources for drinking water, the presence of the Hoor-ol-Azim wetland at the end of the system, and the significant concentration time of water flow from the dam site, establishing optimal operating rule curves for the water resources system and hydro climatic conditions in this basin can effectively alleviate damages caused by floods and droughts in the downstream area.

3.2. Karkhe Reservoir

Karkhe Reservoir is an earthen dam with a height of 127 meters, a crown length of 3030 meters, and a useful reservoir volume (after sedimentation) of 3840 million cubic meters. It is the largest earthen dam in Iran and the Middle East, and the lake created by this dam is the largest artificial lake in the country.

The main objectives of constructing this dam are as follows.

- Providing water for irrigating 220 thousand hectares of downstream lands.
- Supplying drinking water.
- Flood control.
- Diverting water from the dam to Abbas Plain through the tunnel.

- Generating hydropower.

Figures 5 and 6 illustrate the area-volume-elevation curve and the operating levels of the reservoir. Table 1 provides a comprehensive overview of the long-term monthly statistical parameters of inflow, along with demands for various sectors including agriculture, industry, and domestic use.

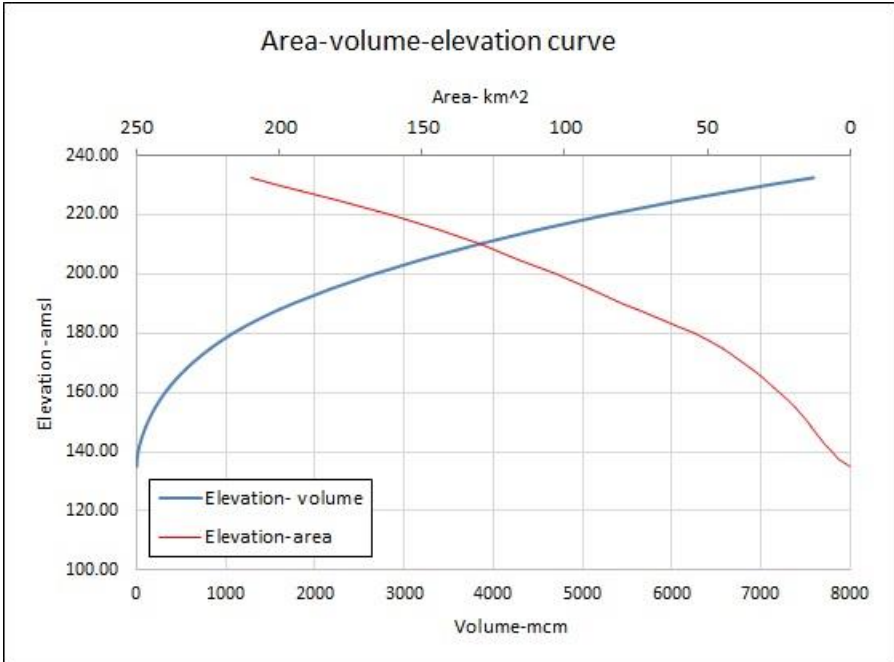


Figure 5. The area-volume-elevation curve of Karkhe reservoir.

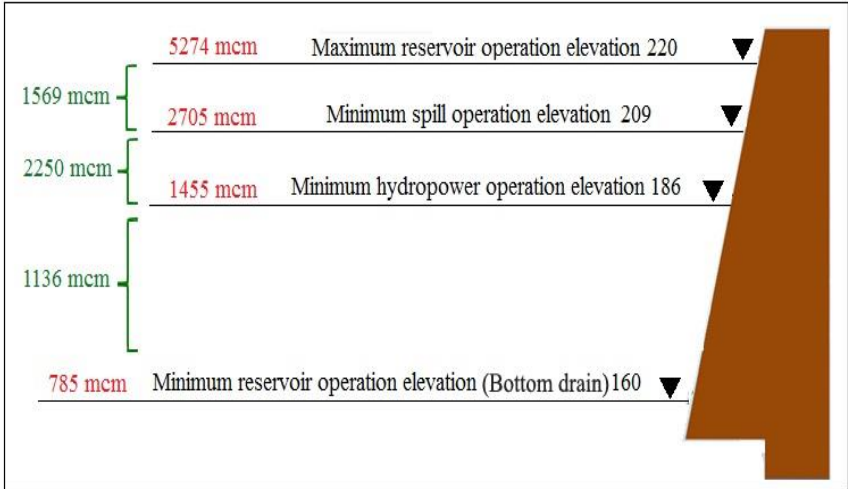


Figure 6. The operating levels of the reservoir.

Table 1. Statistical parameters of inflow, along with demands for various sectors.

Month	Inflow (mcm)				Demand (mcm)				
	Min	Max	Average	Standard deviation	Municipal	Agriculture	Industrial	Environment	Abbas plain
1	12	232	120	56	13	271	9	50	9
2	0	1291	228	182	13	296	5	50	8
3	35	2952	385	386	13	241	3	50	2
4	33	1090	399	231	13	171	3	50	7
5	49	1695	543	371	13	235	5	50	9
6	48	2417	710	482	13	353	14	50	12
7	83	3529	1037	774	13	295	14	100	9
8	57	2263	762	542	13	110	9	100	4
9	29	1401	311	259	13	211	12	100	1
10	20	1103	171	150	13	402	12	100	5
11	0	446	123	81	13	445	12	100	12
12	5	318	109	65	13	354	13	100	13

3.3. Cultivation Pattern

In this basin, summer cultivation (July to the first half of November) covers about 30%, and autumn cultivation (The second half of November to May) covers 70% of crops. Therefore, according to this issue, the priority of water resource planning is to maintain strategic reserves of water resources for autumn crops. The main challenge in meeting the water demands from September to November (before the rains start) is the overlapping water demands of summer crops with the start of autumn crops, which causes double pressure on the limited water resources available. In this period, in addition to the demands of summer crops, land preparation stages and cultivation of beet, canola, and autumn crops are also added to the water demands.

4. Results

4.1. Drought Karkhe Model

For the preparation of the Karkhe rule curve, 6 hedging phases were defined (Figure 7). The demands of the Karkhe reservoir include the demands of Khuzestan and Ilam provinces. It should be noted that the water transfer to Ilam province is done through a tunnel. The elevation of the tunnel is 177 amsl (equivalent to the volume of 927.34 million cubic meters). Below this elevation, there is no possibility of supplying water to the Ilam provinces.

- If the available water level (including reservoir storage and river inflow) is between 160 amsl and V6, we are in the sixth phase of hedging and "a" percent of the downstream demand of Karkhe will be supplied.
- If the available water level (including reservoir storage and river inflow) is between V6 and V5, we are in the fifth phase of hedging and "b" percent of the downstream demand of Karkhe will be supplied.
- If the available water level (including reservoir storage and river inflow) is between V5 and V4, we are in the fourth phase of hedging and "c" percent of the downstream demand of Karkhe will be supplied.
- If the available water level (including reservoir storage and river inflow) is between V4 and V3, we are in the third phase of hedging and "d" percent of the downstream demand of Karkhe will be supplied.
- If the available water level (including reservoir storage and river inflow) is between V3 and V2, we are in the second phase of hedging and "e" percent of the downstream demand of Karkhe will be supplied.
- If the available water level (including reservoir storage and river inflow) is between V2 and V1, we are in the first phase of hedging and "f" percent of the downstream demand of Karkhe will be supplied.
- If the available water level (including reservoir storage and river inflow) is between V1 and 220 amsl, we are in the full supply phase and all the downstream demand of Karkhe will be supplied.
-

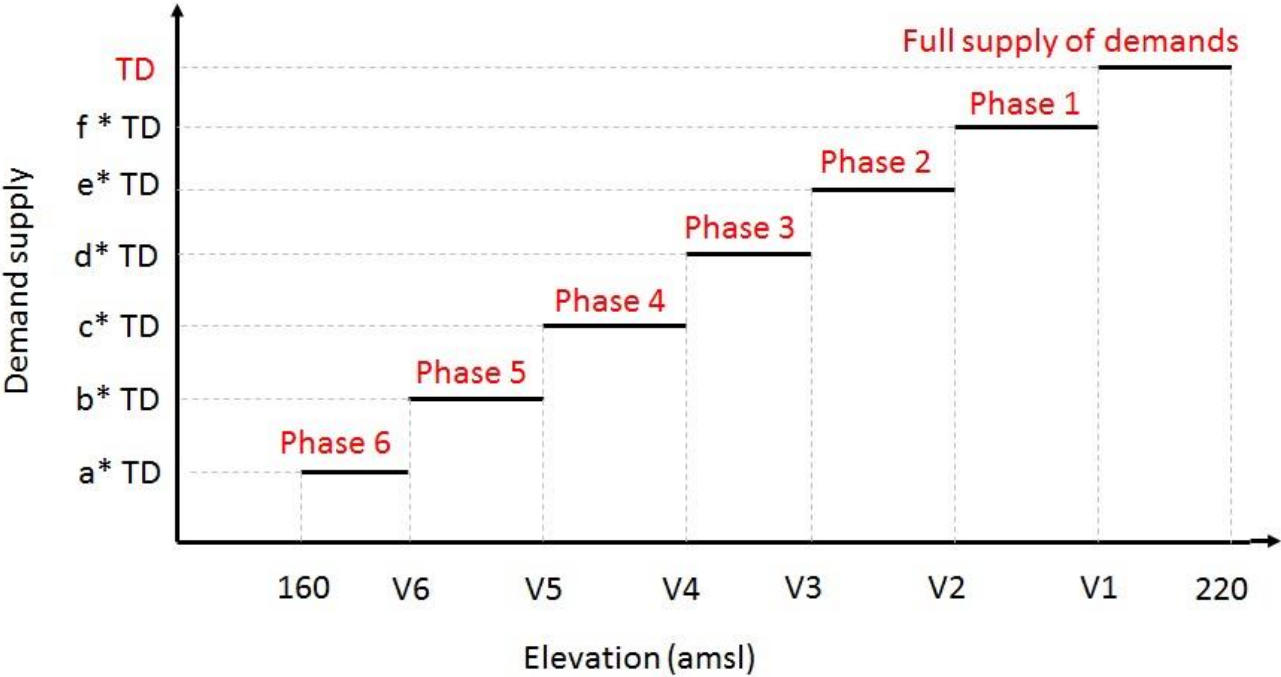


Figure 7. Discrete hedging rule for Karkhe.

The decision variables are.

- V1 to V6: These elevations (12*6=72) are optimized for each month by the program and determine the supply levels.
- A to f: These percentages (12*6=72) are optimized for each month by the program and determine the supply percentages.
- C' to f': The percentage of Abbas plain supply demands for each month and for the first to the fourth phase of hedging (12*4=36).

The objective function is.

$$\text{Min}Z=[W_1*\sum_{y=1}^n\sum_{t=1}^T\beta_t*(\frac{TD_{y,t}-R_{y,t}}{TD_{y,t}})^2+W_2*\sum_{y=1}^n\sum_{t=1}^T(\frac{HP_{max}-HP_{y,t}}{HP_{max}})^2]*\text{Penalty}\tag{13}$$

In this equation, TD is the downstream demand and R is release. Considering that the objective function is minimization, the penalty is considered to be a very large number so that the objective function becomes a large value in situations that are not desirable according to the restrictions and conditions.

HP_{max} is the maximum hydropower energy and HP is the produced hydropower energy. W1 and W2 are coefficients related to the priority of agriculture and hydropower coefficients ($W_1+W_2=1$). Given the cultivation pattern and the significance of autumn cultivation in the basin, the program prioritizes meeting the demands from December to May, with particular emphasis on December and March. The coefficient β_t is considered for this purpose.

During December through the end of May, the minimum hedging phase will be determined by the month of December. This implies that the chosen hedging phase in December cannot drop to a lower phase in the subsequent months until the end of May (December, February, March, April, and May). The reason is that the farmer's planning for cultivation is based on the water released in December. However, in case of rain and an increase in water level, it is possible to go to higher levels of supply.

Calculating hydropower requires knowledge of the reservoir elevation at the start and end of a given period. To account for the unknown end-of-period storage levels, a loop is utilized for each period. The same method is used to calculate evaporation.

The models were developed and tested using 68 years of monthly measured data. The initial 47 years of monthly data were utilized in optimization mode to derive the operation rules, while the remaining 11 years were used for evaluation.

Figure 8 depicts the elevations that delineate the different stages of hedging.

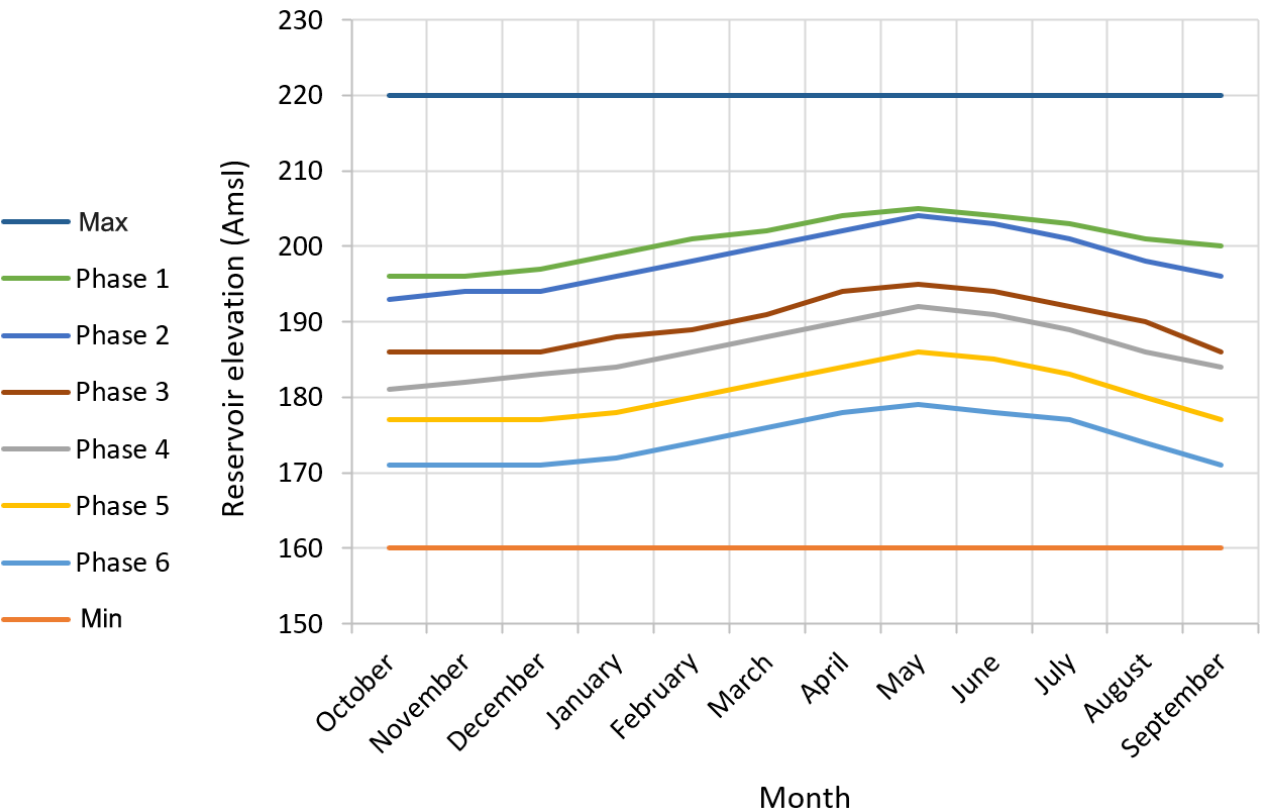


Figure 8. The elevations that delineate the different stages of hedging.

The decision variables for each month, including levels for each phase, supply percentages, and supply volume for two available demand sites (Karkhe and Abbas Plain), are displayed in Table 2. According to the table, the results for example for the month of December are as follows:

- Phase 1: If the water level at the beginning of the period is between 160 and 171 amsl, 40% of the Karkhe demand (123 mcm) will be released.
- Phase 2: If the water level at the beginning of the period is between 171 and 177 amsl, 41% of the Karkhe demand (126 mcm) will be released.
- Phase 3: If the water level at the beginning of the period is between 177 and 183 amsl, 51% of the Karkhe demand (157 mcm) and 12% of the Abbas plain demand (0.3 mcm) will be released.
- Phase 4: If the water level at the beginning of the period is between 183 and 186 amsl, 58% of the Karkhe demand (179 mcm) and 13% of the Abbas plain demand (0.3 mcm) will be released.
- Phase 5: If the water level at the beginning of the period is between 186 and 194 amsl, 84% of the Karkhe demand (259 mcm) and 22% of the Abbas plain demand (0.5 mcm) will be released.
- Phase 6: If the water level at the beginning of the period is between 194 and 197 amsl, 88% of the Karkhe demand (271 mcm) and 87% of the Abbas plain demand (1.9 mcm) will be released.
- If the available water level at the beginning of the period is more than 197 amsl, 100% of the Karkhe demand (310 mcm) and 100% of the Abbas plain demand (2.1 mcm) will be released.

It is calculated in the same way for other months.

Table 2. Levels for each phase, supply percentages, and supply volume for Karkhe downstream.

Phase	Lower level	%	mcm	Lower level	%	mcm	Lower level	%	mcm	Lower level	%	mcm
	Oct.			Nov.			Dec.			Jan.		
6	160	20	69	160	40	146	160	40	123	160	40	95
5	171	20	69	171	41	149	171	41	126	172	41	97
4	177	20	69	177	51	186	177	51	157	178	51	121
3	181	20	69	182	58	211	183	58	179	184	58	137
2	186	31	106	186	84	306	186	84	259	188	84	199
1	193	46	158	194	88	320	194	88	271	196	88	209
Full	196	100	343	196	100	364	197	100	308	199	100	237
	Feb.			Mar.			Apr.			May		
6	160	40	121	160	40	172	160	40	169	160	40	93
5	174	41	124	176	41	176	178	41	173	179	41	95
4	180	51	155	182	51	219	184	51	215	186	51	118
3	186	58	176	188	58	249	190	58	245	192	58	135
2	189	84	255	191	84	361	194	84	354	195	84	195

1	198	88	267	200	88	378	202	88	371	204	88	204
Full	201	100	303	202	100	430	204	100	422	205	100	232
	Jun.			Jul.			Aug.			Sep.		
6	160	20	62	160	20	100	160	20	109	160	20	91
5	178	20	62	177	20	100	174	20	109	171	20	91
4	185	20	62	183	20	100	180	20	109	177	20	91
3	191	20	62	189	20	100	186	20	109	184	20	91
2	194	31	96	192	31	156	190	31	169	186	31	141
1	203	46	143	201	46	231	198	46	251	196	46	209
Full	204	100	311	203	100	502	201	100	545	200	100	454

In order to evaluate the results, the values obtained from the model in the test periods were compared with the SOP method and what has been done in reality. [Tables 3](#) and [4](#) display the monthly vulnerability indexes for the test period.

Table 3. Vulnerability index obtained from the model, sop and operated values for 2011-2016.

Month	Year	SOP	Model	Operated	Year	SOP	Model	Operated	year	SOP	Model	Operated
Oct	2011-12	0.03	0.65	0.65	2012-13	0.96	0.65	0.75	2013-14	1.00	0.65	0.58
Nov		0.02	0.52	0.56		0.66	0.53	0.73		0.98	0.53	0.71
Dec		0.01	0.47	0.38		0.23	0.52	0.88		0.89	0.52	0.65
Jan		0.03	0.47	0.26		0.50	0.53	0.71		0.53	0.53	0.57
Feb		0.48	0.47	0.54		0.03	0.53	0.40		0.42	0.53	0.66
Mar		0.80	0.47	0.55		0.03	0.53	0.43		0.35	0.53	0.50
Apr		0.63	0.47	0.62		0.02	0.53	0.60		0.39	0.53	0.66
May		0.57	0.48	0.57		0.10	0.53	0.62		0.02	0.53	0.51
Jun		0.56	0.86	0.75		0.51	0.64	0.65		0.00	0.64	0.66
Jul		0.90	0.86	0.84		0.58	0.65	0.61		0.72	0.65	0.67
Aug		0.96	0.86	0.84		0.87	0.65	0.60		0.89	0.65	0.62
Sep		0.99	0.86	0.81		1.00	0.65	0.59		0.94	0.65	0.65
Avg.		0.50	0.62	0.62		0.46	0.58	0.63		0.59	0.58	0.62
Oct	2014-15	1.00	0.74	0.58	2015-16	1.00	0.91	0.88	2016-17	0.03	0.03	0.13
Nov		0.99	0.66	0.56		0.94	0.53	0.87		0.02	0.13	0.16
Dec		0.64	0.58	0.50		0.39	0.52	0.61		0.01	0.12	0.19
Jan		0.55	0.59	0.44		0.03	0.53	0.68		0.03	0.14	0.10
Feb		0.77	0.61	0.61		0.03	0.53	0.33		0.03	0.14	0.00
Mar		0.83	0.68	0.72		0.03	0.53	0.53		0.03	0.14	0.20
Apr		0.72	0.53	0.80		0.02	0.53	0.60		0.02	0.13	0.25
May		0.50	0.55	0.75		0.02	0.13	0.00		0.02	0.13	0.08
Jun		0.80	0.96	0.85		0.00	0.00	0.00		0.00	0.58	0.19
Jul		0.94	0.96	0.90		0.01	0.01	0.37		0.01	0.14	0.22
Aug		0.97	0.96	0.89		0.02	0.02	0.35		0.02	0.59	0.25
Sep		0.97	0.96	0.91		0.03	0.03	0.14		0.03	0.59	0.32
Avg.		0.81	0.73	0.71		0.21	0.36	0.45		0.02	0.24	0.17

The severity of a failure is indicated by its vulnerability. A higher coefficient value indicates a greater vulnerability of the system. As anticipated, the SOP method falls short in delivering desirable outcomes due to its limited approach. It lacks the required foresight for effective operation management. As previously noted, the farmer's cultivation is dependent on the water received at the start of the cultivation period. Hence, the fluctuation of vulnerability percentage during the cultivation months leads to losses and is unfavorable. Moreover, the period spanning from December to May, with particular emphasis on December and March, is more susceptible to water scarcity. As the results indicate, the program has effectively reduced the shortage in these months and reallocated it to other months. Also, the optimized operational policy remains consistent across similar periods in different water years, promoting greater system stability. Furthermore, the operational policy remains more consistent during similar periods within a water year (November to May and June to October).

Table 4. Vulnerability index obtained from the model, sop and operated values for 2016-2022.

Month	Year	SOP	Model	Operated	Year	SOP	Model	Operated	Year	SOP	Model	Operated
Oct	2017-18	0.03	0.59	0.08	2018-19	0.85	0.59	0.09	2019-20	0.03	0.03	0.00
Nov		0.02	0.13	0.30		0.86	0.13	0.61		0.02	0.02	0.04
Dec		0.01	0.12	0.02		0.92	0.12	0.53		0.01	0.01	0.23
Jan		0.03	0.14	0.00		0.03	0.14	0.00		0.03	0.03	0.00
Feb		0.03	0.14	0.11		0.03	0.03	0.00		0.03	0.03	0.00
Mar		0.03	0.14	0.34		0.03	0.00	0.00		0.03	0.00	0.00
Apr		0.02	0.13	0.41		0.02	0.00	0.00		0.02	0.00	0.00
May		0.02	0.13	0.41		0.02	0.00	0.00		0.02	0.00	0.00
Jun		0.00	0.64	0.53		0.00	0.00	0.00		0.00	0.00	0.00
Jul		0.01	0.58	0.34		0.01	0.01	0.00		0.01	0.01	0.00
Aug		0.02	0.59	0.28		0.02	0.02	0.00		0.02	0.02	0.00

Sep		0.03	0.59	0.25		0.03	0.03	0.00		0.03	0.03	0.00
Avg.		0.02	0.33	0.26		0.23	0.09	0.10		0.02	0.01	0.02
Oct	2020-21	0.03	0.03	0.00	2021-22	0.83	0.65	0.00				
Nov		0.02	0.04	0.06		0.41	0.13	0.20				
Dec		0.01	0.12	0.38		0.86	0.36	0.12				
Jan		0.03	0.14	0.00		0.62	0.36	0.55				
Feb		0.03	0.14	0.00		0.95	0.36	0.25				
Mar		0.03	0.14	0.03		0.96	0.36	0.25				
Apr		0.02	0.13	0.21		0.90	0.36	0.38				
May		0.02	0.13	0.17		0.23	0.36	0.51				
Jun		0.00	0.58	0.46		0.91	0.71	0.74				
Jul		0.01	0.58	0.42		0.95	0.71	0.82				
Aug		0.53	0.59	0.31		0.96	0.71	0.87				
Sep		0.88	0.59	0.29		0.95	0.71	0.88				
Avg.		0.13	0.27	0.19		0.79	0.48	0.46				

As previously mentioned, December marks the start of autumn cultivation, and the water level is crucial during this time. Table 5 displays the water level at the beginning of December. It is evident that if the model was used as an operational policy, the average level at the start of December would be 193 meters above sea level. However, in actuality, the average balance at the beginning of this month was 187.

Table 5. Water level at the beginning of the December.

Water year	SOP	Model	Operated
2011-12	181	184	182
2012-13	160	178	181
2013-14	160	180	183
2014-15	160	178	181
2015-16	161	180	188
2016-17	197	199	201
2017-18	178	199	197
2018-19	166	200	203
2019-20	202	210	197
2020-21	199	210	183
2021-22	164	208	172
Average	175	193	188

4.2. Flood Karkhe Model

After utilizing the multi-step flow method to identify the operational pattern of Karkhe during floods, as explained in the methodology section, and implementing several optimizations, the distinct discharges from various levels were determined. Based on these discharges, flood routing with different return periods was carried out. Table 6 shows the discharge results from various levels of Karkhe, and Table 7 provides a summary of the flood routing outcomes. The tables show that the maximum discharge from the Karkhe reservoir for the return periods of 2, 5, 10, 20, and 25 years are 650, 994, 994, 994, and 1232 cubic meters per second, respectively. Thus, the flow rates for various stages have been determined to ensure the stability and safety of the dam. It should be noted that for convenience, the optimized flow rates have been converted to Rand numbers. Figure 9 shows the results of flood routing with various return periods.

Table 6. Output flow from different levels.

No.	Water level	The maximum flow through the spillway in the state of fully open valve	The maximum flow obtained from the optimization	Final flow rate
	m	m³/s	m³/s	m³/s
1	220	6558	650	650
2	221	7469	994	1000
3	222	8486	1232	1250
4	223	9446	1366	1400
5	224	10411	1798	1800
6	225	11432	2500	2500
7	226	12399	6000	6000
8	227	13379	12000	12000
9	228	14461	14000	14000

Table 7. Summary of the flood routing outcomes.

Return Period	Maximum inflow	Maximum outflow	Water level
	m ³ /s	m ³ /s	amsl
2	1680	650	220.36
5	2650	994	221
10	3360	994	221.31
20	4090	994	221.86
25	4430	1232	222.03
50	5032	1232	222.48
100	5864	1366	223.1
200	6719	1366	223.86
500	7881	1798	224.42
1000	8797	2500	225
10000	12336	6000	226

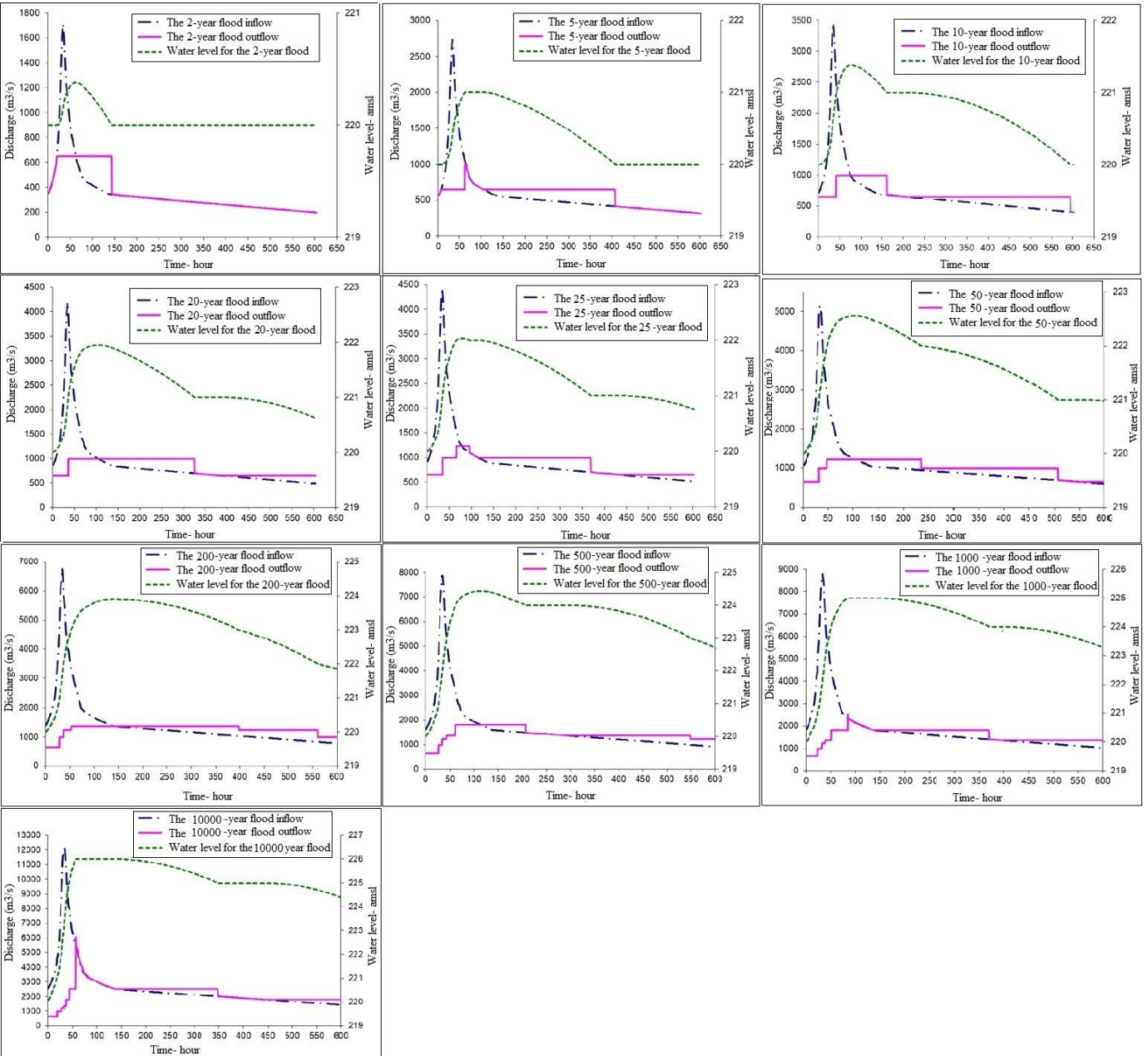


Figure 9. Flood routing results for different return periods.

As evident from the tables and figures, the larger the flood entering the reservoir, the higher the water level in the reservoir will rise, and correspondingly, the outflow from the spillway should also increase in proportion to the rise in water level in the reservoir. For example, the maximum water level of the reservoir per flood with a return period of 50 years with a peak input of 5032 cubic meters per second is equal to 222.48 meters from the sea level. Therefore, the maximum discharge from the reservoir for this flood is equal to the discharge of the third step (distance between 222 and 223 meters above the sea level), i.e. 1232 cubic meters per second.

In April 2018, two heavy rainfall systems occurred in the Karkhe watershed with a time interval of 4 days. The heavy rain resulted in a destructive flood in the Karkhe basin and its surrounding cities. The hydrograph of this flood was analyzed to determine the final results and flow for various stages (Figure 10). The figure shows that using the presented method, the maximum discharge from the Karkhe during the 2018 flood would be 2500 cubic meters per second and the reservoir water level would reach 225 meters above sea level. These numbers align closely with the actual discharge and water level during the historical April 2018 flood.

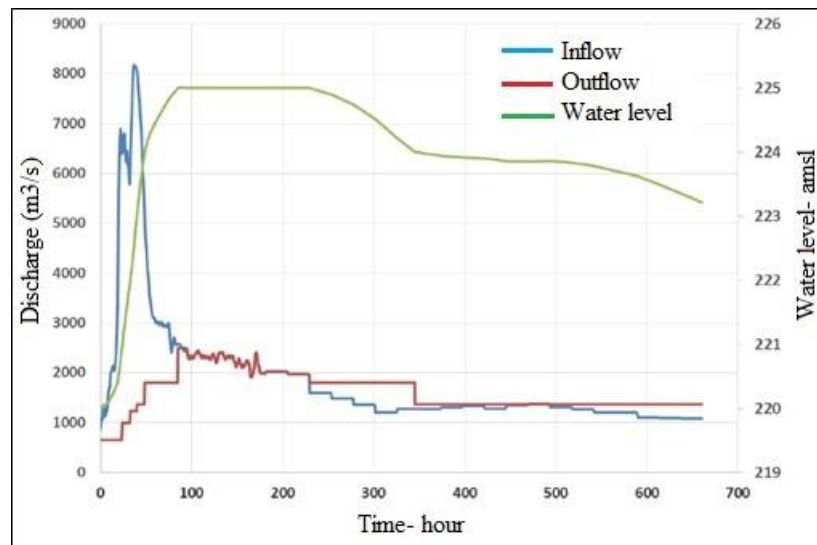


Figure 10. April 2018 flood routing.

5. Conclusion

The study introduced a simulation-optimization model to find the best rule curve for the Karkhe reservoir in floods and droughts. During droughts, the model used a hedging approach to distribute shortages in less critical periods, preventing severe shortages in crucial times. In floods, the model routed floods with various return periods (2 to 10000) while ensuring maximum reservoir capacity utilization without downstream damage. A multi-stage flood routing method was used for this. It should be noted that the constraints and model structure were determined based on unique conditions of the Karkhe basin, including irregular water distribution, extensive domestic and agricultural water usage, various and conflicting cultivation patterns, susceptibility to flooding, and significant changes in the upstream and downstream areas, including alterations in shape and water resource utilization, as well as changes in the rivers' morphological condition and water carrying capacity.

References

- [1] T. Thongwan, A. Kangrang, and H. Prasanchum, "Multi-objective future rule curves using conditional tabu search algorithm and conditional genetic algorithm for reservoir operation," *Heliyon*, vol. 5, no. 9, 2019. <https://doi.org/10.1016/j.heliyon.2019.e02401>
- [2] M. Bayesteh and A. Azari, "Stochastic optimization of reservoir operation by applying hedging rules," *Journal of Water Resources Planning and Management*, vol. 147, no. 2, p. 04020099, 2021. [https://doi.org/10.1061/\(asce\)wr.1943-5452.0001312](https://doi.org/10.1061/(asce)wr.1943-5452.0001312)
- [3] T. Hashimoto, J. R. Stedinger, and D. P. Loucks, "Reliability, resiliency, and vulnerability criteria for water resource system performance evaluation," *Water Resources Research*, vol. 18, no. 1, pp. 14-20, 1982. <https://doi.org/10.1029/wr018i001p00014>
- [4] M. Bayazit and N. Ünal, "Effects of hedging on reservoir performance," *Water Resources Research*, vol. 26, no. 4, pp. 713-719, 1990. <https://doi.org/10.1029/wr026i004p00713>
- [5] J.-S. Shih and C. ReVelle, "Water-supply operations during drought: Continuous hedging rule," *Journal of Water Resources Planning and Management*, vol. 120, no. 5, pp. 613-629, 1994. [https://doi.org/10.1061/\(asce\)0733-9496\(1994\)120:5\(613\)](https://doi.org/10.1061/(asce)0733-9496(1994)120:5(613))
- [6] J.-S. Shih and C. ReVelle, "Water supply operations during drought: A discrete hedging rule," *European Journal of Operational Research*, vol. 82, no. 1, pp. 163-175, 1995. [https://doi.org/10.1016/0377-2217\(93\)e0237-r](https://doi.org/10.1016/0377-2217(93)e0237-r)
- [7] M. Zargar, H. M. Samani, and A. Haghighi, "Optimization of gated spillways operation for flood risk management in multi-reservoir systems," *Natural Hazards*, vol. 82, pp. 299-320, 2016. <https://doi.org/10.1007/s11069-016-2202-7>
- [8] N. Acanal and T. Haktanir, "Five-stage flood routing for gated reservoirs by grouping floods into five different categories according to their return periods," *Hydrological sciences journal*, vol. 44, no. 2, pp. 163-172, 1999. <https://doi.org/10.1080/02626669909492215>
- [9] N. Acanal, R. Yurtal, and T. Haktanir, "Multi-stage flood routing for gated reservoirs and conjunctive optimization of hydroelectricity income with flood losses," *Hydrological Sciences Journal*, vol. 45, no. 5, pp. 675-688, 2000. <https://doi.org/10.1080/02626660009492370>
- [10] T. Haktanir and Ö. Kisi, "Ten-stage discrete flood routing for dams having gated spillways," *Journal of Hydrologic Engineering*, vol. 6, no. 1, pp. 86-90, 2001. [https://doi.org/10.1061/\(asce\)1084-0699\(2001\)6:1\(86\)](https://doi.org/10.1061/(asce)1084-0699(2001)6:1(86))
- [11] F. Salehi, M. Najarchi, M. M. Najafizadeh, and M. M. Hezaveh, "Multistage models for flood control by gated spillway: Application to Karkheh dam," *Water*, vol. 14, no. 5, p. 709, 2022. <https://doi.org/10.3390/w14050709>
- [12] C. Su *et al.*, "An MILP based optimization model for reservoir flood control operation considering spillway gate scheduling," *Journal of Hydrology*, vol. 613, p. 128483, 2022. <https://doi.org/10.1016/j.jhydrol.2022.128483>
- [13] Z. W. Geem, J. H. Kim, and G. V. Loganathan, "A new heuristic optimization algorithm: Harmony search," *Simulation*, vol. 76, no. 2, pp. 60-68, 2001.
- [14] J. H. Kim, Z. W. Geem, and E. S. Kim, "Parameter estimation of the nonlinear muskingum model using harmony search 1," *JAWRA Journal of the American Water Resources Association*, vol. 37, no. 5, pp. 1131-1138, 2001.
- [15] K. S. Lee and Z. W. Geem, "A new meta-heuristic algorithm for continuous engineering optimization: Harmony search theory and practice," *Computer Methods in Applied Mechanics and Engineering*, vol. 194, no. 36-38, pp. 3902-3933, 2005. <https://doi.org/10.1016/j.cma.2004.09.007>
- [16] M. Mahdavi, M. Fesanghary, and E. Damangir, "An improved harmony search algorithm for solving optimization problems," *Applied Mathematics and Computation*, vol. 188, no. 2, pp. 1567-1579, 2007. <https://doi.org/10.1016/j.amc.2006.11.033>
- [17] M. G. Omran and M. Mahdavi, "Global-best harmony search," *Applied mathematics and computation*, vol. 198, no. 2, pp. 643-656, 2008. <https://doi.org/10.1016/j.amc.2007.09.004>
- [18] M. Fesanghary, M. Mahdavi, M. Minary-Jolandan, and Y. Alizadeh, "Hybridizing harmony search algorithm with sequential quadratic programming for engineering optimization problems," *Computer Methods in Applied Mechanics and Engineering*, vol. 197, no. 33-40, pp. 3080-3091, 2008. <https://doi.org/10.1016/j.cma.2008.02.006>

- [19] S. Ashrafi and A. Dariane, "Performance evaluation of an improved harmony search algorithm for numerical optimization: Melody search (MS)," *Engineering Applications of Artificial Intelligence*, vol. 26, no. 4, pp. 1301-1321, 2013. <https://doi.org/10.1016/j.engappai.2012.08.005>
- [20] A. B. Dariane and F. Karami, "Deriving hedging rules of multi-reservoir system by online evolving neural networks," *Water Resources Management*, vol. 28, pp. 3651-3665, 2014. <https://doi.org/10.1007/s11269-014-0693-0>
- [21] A. Dariane, M. Ghasemi, F. Karami, A. Azaranfar, and S. Hatami, "Crop pattern optimization in a multi-reservoir system by combining many-objective and social choice methods," *Agricultural Water Management*, vol. 257, p. 107162, 2021. <https://doi.org/10.1016/j.agwat.2021.107162>
- [22] F. Karami and A. B. Dariane, "Melody search algorithm using online evolving artificial neural network coupled with singular spectrum analysis for multireservoir system management," *Iranian Journal of Science and Technology, Transactions of Civil Engineering*, vol. 46, no. 2, pp. 1445-1457, 2022.